ELSEVIER

Journal of Power Sources 96 (2001) 321–328

JOURNAL OF POWER SOURCES

www.elsevier.com/locate/jpowsour

# Symmetric cell approach and impedance spectroscopy of high power lithium-ion batteries

C.H. Chen, J. Liu, K. Amine*

*Argonne National Laboratory, Electrochemical Technology Program, Chemical Technology Division, Argonne, IL 60439, USA*

Received 30 October 2000; accepted 5 November 2000

**Abstract**

High power lithium-ion cells are a very promising energy source for practical hybrid vehicles. It is found that the impedance of the 18650 high-power cells using $LiNi_{0.8}Co_{0.2}O_2$ chemistry increases with time during the beginning period of storage. A symmetric cell approach is developed to distinguish the anode and cathode effects on the impedance rise. Cathode impedance, especially charge-transfer resistance, is identified as the main component of the cell impedance and is most responsible for the rise of the cell impedance during storage at room temperature. With analysis of impedance spectra from a variety of cells, the charge-transfer process is thought to take place at the interface between the electrolyte solution and the surface of surface layers on the electrode. We also propose that the surface layers might be mixed conductors of electrons and lithium ions, instead of pure lithium-ion conductors. The nature of the surface layers on the cathode is likely different from that of the surface layers on the anode. 

*Keywords:* Impedance spectroscopy; Lithium-ion batteries; Electrode process

## 1. Introduction

Rechargeable lithium-ion batteries using 4 V cathodes (e.g. $LiCoO_2$ or $LiNi_{0.8}Co_{0.2}O_2$) and carbon anode (various graphite and mixtures) have been studied for many years [1–4] and commercialized by several companies (e.g. Sony and Panasonic). Owing to their inherent high energy density and environment-friendly characteristics, they are rapidly taking over the markets for other battery products (such as lead-acid and alkaline batteries) for applications in consumer electronics. At present, industry and academic R&D efforts in this field focus on improving the performance of current battery systems and further lowering the manufacturing cost. Apart from these applications, lithium-ion batteries are expected to find very important applications in zero-emission electric vehicles and high-fuel-efficiency hybrid vehicles. Such uses require high power lithium-ion batteries packaged in a small volume (i.e. high power density) [5,6]. Fabrication and evaluation of high-power lithium-ion batteries are the main focus areas for Argonne's battery research group.

In the course of that work, we made high-power cylindrical lithium-ion batteries with a reversible 10 C rate capacity of 1 A h and 18650 size (18 mm in diameter and 65 mm long). After screening various electrode materials [7], we chose $LiNi_{0.8}Co_{0.2}O_2$ as the active cathode material and a mixture of two different kinds of graphite as the anode (see next section for details). We found (Fig. 1) that the freshly charged batteries will experience significant impedance rise during the first 3 weeks or so of storage and then maintain a stable impedance. This impedance change happens not only for full charge but also for other states of charge. To find out the cause of this impedance rise, laboratory-scale cells using the same electrodes and electrolyte were investigated by ac impedance technique in this study. A new approach based on the use of symmetric cells was proposed to clearly distinguish the contribution from cathode and anode processes [8]. In this approach, two normal cells are made into two symmetric cells by swapping the anode of one with the cathode of the other. The cathode processes, especially the charge-transfer process, were found to be the main source of the impedance change.

## 2. Experimental

The Argonne 18650 lithium-ion cells were made of a multi-fold cathode laminate, a separator, and an anode laminate. The cathode laminate was composed of 84%

* Corresponding author. Tel.: +1-630-252-3838; fax: +1-630-252-4176.
*E-mail address*: amine@cmt.anl.gov (K. Amine).

0378-7753/01/$ – see front matter 
PII: S0378-7753(00)00666-2

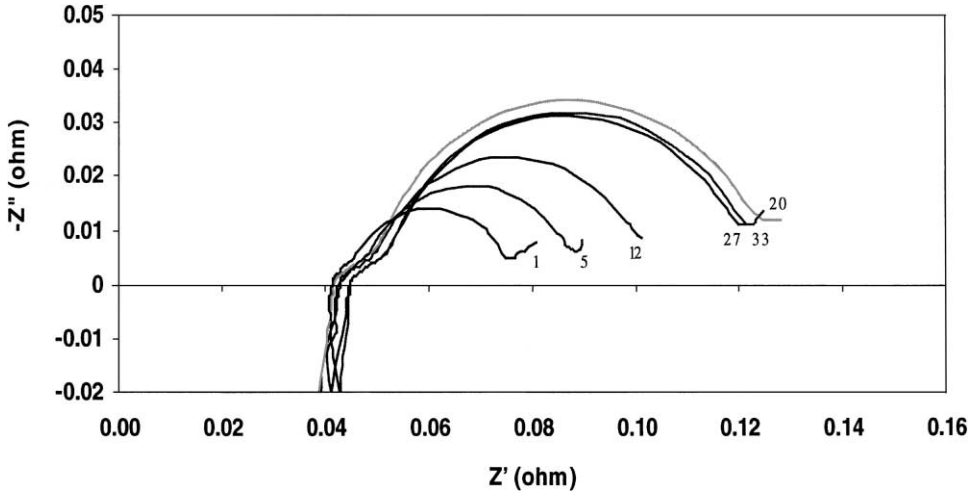


Fig. 1. An ac impedance spectra of an Argonne 18650 lithium-ion cell as a function of storage time. Numbers on the spectrum indicate days of storage.

$LiNi_{0.8}Co_{0.2}O_2$, 8% mixed carbon additive and 8% polyvinylidene fluoride (PVDF) binder with about 35% porosity on 21 μm thick aluminum foil. The anode laminate was composed of 75% MCMB-6 graphite, 16% SFG-6 graphite, and 9% PVDF binder on 15 μm thick copper foil. Both the cathode and anode laminates were prepared on an industrial processing line so that excellent uniformity of the electrodes was insured. The electrolyte was ethylene carbonate (EC)/diethyl carbonate (DEC)/1 M lithium hexafluorophosphate ($LiPF_6$-Merck LP40). A porous PE membrane (37 μm thick, Celgard) was used as the separator. Our laboratory-scale cells were assembled into stainless steel fixtures (32 $cm^2$) in an helium-filled glove box and hermetically sealed. For these laboratory-scale cells, the electrode laminates were punched to 20.3 or 15.5 $cm^2$ and 37 μm thick separator was used. It should be noted that the capacity of the lithium-ion cells made from these laminates was cathode-limited.

The ac impedance of the cells was measured by using a Schlumberger model 1255 frequency response analyzer connected to a Schlumberger model 1286 electrochemical interface and a EG&G PAR 273 potentiostat. A small (20 mV) ac perturbation plus a dc bias voltage equal to the cell open-circuit-voltage (OCV) was applied with a frequency sweep from 0.01 Hz to 100 kHz during measurement. One fully charged 18650 cell and one fully charged laboratory-scale cell were tested, with impedance measured as function of storage time. In addition, two half-charged laboratory-scale cells (3.5 V cut-off) were also tested. These two cells were then opened in the glove box to make two symmetric cells: the cathode of one cell was exchanged with the anode of the other cell (Fig. 2). The cathode cell showed an OCV of only a few mV, while the anode cell showed an OCV of about 20 mV. The ac impedance of the symmetric cells was also measured as function of storage time.

To clarify the exact location at which charge-transfer takes place, we designed an experiment based on the symmetric cell approach in which we studied the ac impedance of two fully charged cells with different electrolyte solutions, i.e. 1 M $LiPF_6$ in EC:DEC and 1 M $LiPF_6$ in 2EC:DEC:2DMC (dimethyl carbonate). The two source cells had been stored for about 17 days at room temperature before we made them into two symmetric cells. In addition,

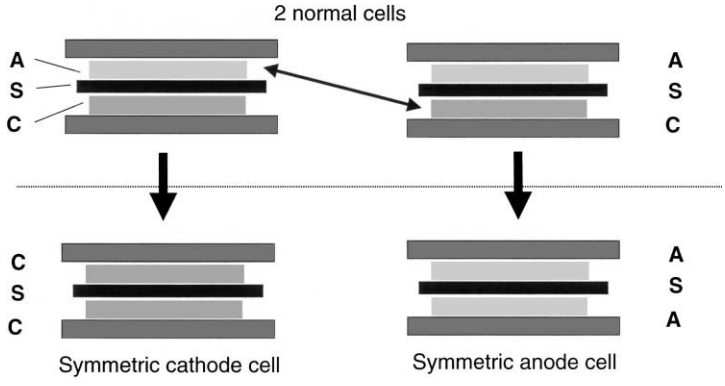


Fig. 2. Scheme of symmetric cell approach. A, S, and C stand for anode, separator, and cathode, respectively.

three fully charged laboratory-scale cells using different electrolytes, i.e. 1 M $LiPF_6$ in EC:DEC, 2EC:DEC:2DMC or EC:4EMC (ethyl methyl carbonate), were also tested.

It was also noticed that, for these symmetric cells, virtually no difference in the impedance spectra was observed after the OCV was brought to 1–2 mV by short-circuiting the cells. Thus, the effect of short-circuiting is negligible and is not discussed below.

## 3. Results and discussions

### 3.1. Impedance of normal cells

Because of its large electrode area (about 600 $cm^2$), an 18650 cell shows a very small total resistance (<0.13 Ω), which allows the detection of the inductive resistance at high frequencies (Fig. 1). This inductance is usually attributed to the leads. On the ac impedance spectra, the high-frequency intercepts at the real axis represent the total impedance component from such virtually zero-time-relaxation processes as electron transport through the electrodes, current collectors and leads, and lithium-ion migration through the liquid electrolyte. Since both electrodes contain highly conducting carbon, the electronic resistances of the electrodes can be neglected. On the basis of the ionic conductivity of the 1 M $LiPF_6$ electrolyte (on the order of $10^{-3}$ S/cm) and the separator thickness (37 μm), the electrolyte resistance may be estimated to be about 0.006 Ω, which is considerably smaller than the intercept values shown in Fig. 1. Therefore, this high-frequency impedance, corresponding to the dc resistance of a very short time pulse, is almost from the leads. The medium-to-low-frequency impedance is about 0.035 Ω on day 1 and increases during the first 3 weeks of storage.

The impedance spectra of a laboratory-scale cell as function of storage time are shown Fig. 3. The trend observed in the 18650 cell is also seen in the laboratory cell, confirming the increase in cell impedance during the beginning of storage period. Note that the inductive behavior and relatively large intercept at the high-frequency end do not appear here because the contribution from the leads is

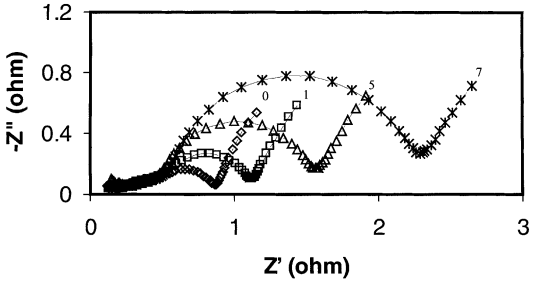


Fig. 3. An ac impedance spectra of a laboratory-scale lithium-ion cell during storage. Numbers on the spectrum indicate days of storage. The electrode area was 20.3 $cm^2$; the electrolyte solvent was EC:DEC.

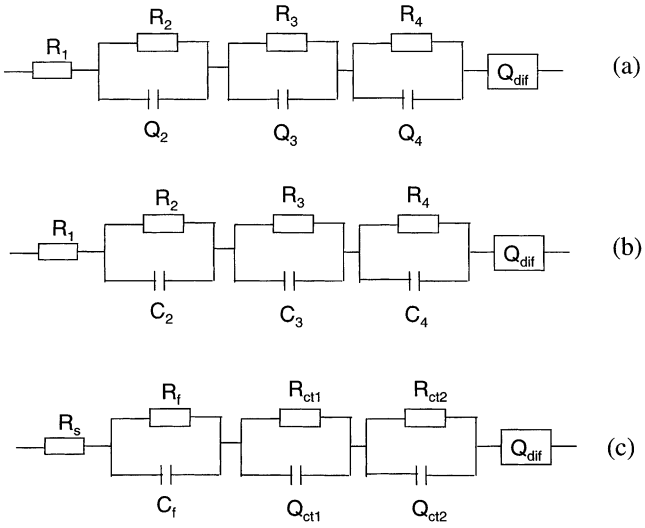


Fig. 4. Three possible equivalent circuit analogs for a lithium-ion cell. *R*, *C*, and *Q* stand for resistor, capacitor, and constant phase element, respectively. The subscripts s, f, ct, and dif stand for the electrolyte solution, surface layer, charge-transfer, and diffusional component, respectively.

negligible in the case of a small cell. Each of the impedance spectra is composed of at least three semicircles in the high-to-medium frequency range and a straight line at low frequencies. The straight line is probably related to lithium-ion diffusion in one or both electrodes, while the semicircles should be related to lithium migration through surface films on the electrodes and to the charge-transfer processes between the electrodes and the electrolyte. Following Aurbach and coworkers impedance studies on carbon anodes and 4 V cathodes [9–11], a simplified serial equivalent circuit is proposed for the complete cell and shown in Fig. 4a. Considering the fact that very porous electrodes are used in the cell, the commonly used capacitor *C* in this serial analog is replaced with constant phase elements *Q* given by $Z(Q) = 1/(i\omega T)^m$, where $i = (-1)^{0.5}$, $\omega = 2\pi f$, $T$ is a constant, and $0 < m \leq 1$ [12]. When $m = 1$, *Q* becomes a pure capacitor with *T* as the capacitance. On the other hand, it becomes a Warburg impedance when $m = 0.5$. This equivalent circuit can fit the impedance data with good accuracy, as shown in a fitting example for the impedance spectrum on day 7 (Fig. 5). Notice that $T_2$, $T_3$, and $T_4$ are on the order of $10^{-5}$ F, $10^{-2}$ s $\Omega^{-2.1}$ and $10^{-2}$ s $\Omega^{-1.1}$, respectively. To simplify the physical meanings of $T_2$, $T_3$, and $T_4$ they are assumed to be the capacitors $C_2$, $C_3$, and $C_4$ in the equivalent circuit Fig. 4b. The data-fitting with this modified equivalent circuit achieves good accuracy for the high-to-medium frequency segments (Fig. 5), with $C_2 = 83.7$ μF, $C_3 = 4.26$ mF, and $C_4 = 81$ mF. On the basis of these capacitance values, $R_2Q_2$ in the equivalent circuit Fig. 4a may be reasonably attributed to lithium transport in surface films, and $R_3Q_3$ and $R_4Q_4$ to the charge-transfer processes. Thus, the whole cell can be modeled with the equivalent circuit Fig. 4c, where s stands for electrolyte ($LiPF_6$) solu-

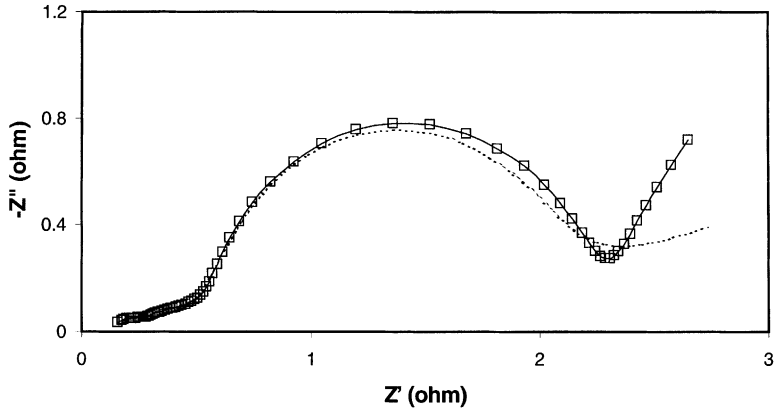


Fig. 5. An ac impedance spectrum of the lithium-ion cell on day 7 of storage (squares) and the simulation results with the equivalent circuits shown in Fig. 4a (solid line) and Fig. 4b (dashed line). The fitting parameters for the solid line are: $R_1 = 0.15\ \Omega$, $R_2 = 0.067\ \Omega$, $T_2 = 59\ \mu F$, $m_2 = 1$, $R_3 = 0.41\ \Omega$, $T_3 = 0.076\ s\ \Omega^{-2.1}$, $m_3 = 0.48$, $R_4 = 1.60\ \Omega$, $T_4 = 0.075\ s\ \Omega^{-1.1}$, $m_4 = 0.95$, $T_{dif} = 7.6\ s\ \Omega^{-1.5}$ and $m_{dif} = 0.66$. The fitting results for the dashed line are: $R_1 = 0.1\ \Omega$, $R_2 = 0.061\ \Omega$, $C_2 = 83.7\ \mu F$, $R_3 = 0.062\ \Omega$, $C_3 = 4.26\ mF$, $R_4 = 1.21\ \Omega$, $C_4 = 81\ mF$, $T_{dif} = 1.22\ s\ \Omega^{-5.5}$ and $m_{dif} = 0.18$.

tion, f for surface films, and ct for charge transfer. Thus, $Q_{ct}$ here may be regarded as a frequency-dependent double-layer capacitor. On the basis of the time constant that $R_{ct2}Q_{ct2}$ corresponds to that medium-to-low frequency semicircle in the impedance spectra.

Fig. 6 shows the values resulting from using equivalent circuit Fig. 4c to fit the spectra from the laboratory-scale cell (Fig. 3). Obviously, the charge-transfer resistance, $R_{ct1}$ and especially $R_{ct2}$, is the main contributor to the cell impedance. Furthermore, the increase in $R_{ct2}$ is most responsible for the rise in the cell impedance with storage time. Therefore, it is important to find out which electrode is the site of the charge-transfer process that is the source of $R_{ct2}$. Additionally, $R_fC_f$ and $Q_{dif}$ of circuit Fig. 4c can only be regarded as the total effect from both electrodes. These issues provided the motivation to develop the symmetric cell approach.

### 3.2. Impedance of symmetric cells

The initial ac impedance spectra of two symmetric cells and their two half-charged source cells are shown in Fig. 7a–c. This symmetric cell approach allows us to study the cathode and anode separately. The summation spectra of the source cells and the symmetric cells are compared in Fig. 7d to confirm the validity of this approach. By comparing the spectrum of the source cells, the symmetric anode cell, and the symmetric cathode cell, it can be concluded that the cathode process is the dominant contributor to the large semicircle observed at medium to low frequencies in the spectra of a complete cell. The other hand, the anode process contributes to the cell impedance to a much lesser extent. A more detailed discussion of this issue is given elsewhere [5]. This cathode effect was also found for the cells with other states of charge. Therefore, $R_{ct2}Q_{ct2}$ in equivalent circuit Fig. 4c can be ascribed to the charge-transfer process at the cathode. To minimize and stabilize the cell impedance, future research must focus on the cathode or the interaction between the cathode and the electrolyte.

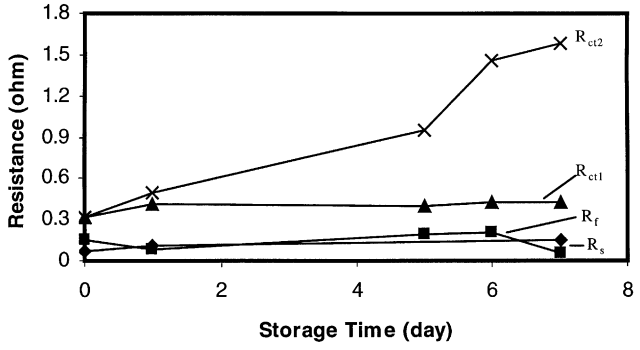


Fig. 6. Fitting results of the lithium-ion cell for the equivalent circuit in Fig. 4c as a function of storage time.

The same two symmetric cells were also monitored for impedance change during room-temperature storage. Three additional representative spectra for each cell are shown in Figs. 8 and 9. The spectra of the symmetric anode cell (Fig. 8) seem to consist of two semicircles and a low-frequency straight line and may be modeled with good accuracy by the circuit shown in Fig. 10a. This circuit is basically a simplified version of the circuit used by Aurbach and Zaban [9]. Only one *RC* pair is used here to model the surface layers. Hence, the change in $R_s$, $R_f$, $R_{ct}$ and $C_f$ for the symmetric anode cell during storage may be derived (Fig. 11). Note that $R_f$ and $R_{ct}$ of a symmetric cell should be twice the resistance values of a single anode in a complete cell, while $C_f$ should be half of the capacitance value. It can be seen that the surface layer resistance ($R_f$) and the electrolyte solution resistance ($R_s$) in the anode cell are very close to each other and both increase with storage time, while the charge-transfer resistance ($R_{ct}$) is about five times larger (Fig. 11a). The increase in $R_f$ may be explained by the increase in the surface layer thickness with the formation of more surface layers during storage. The mechanism for

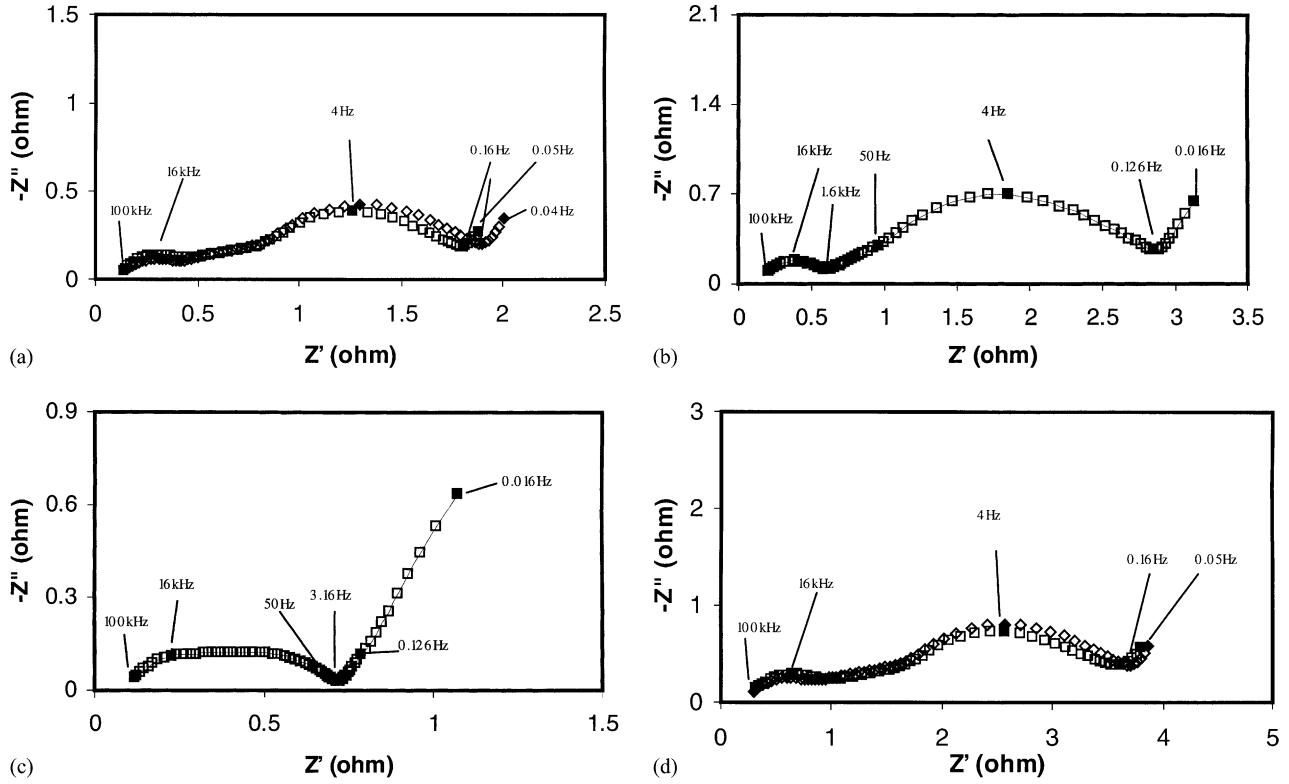


Fig. 7. An ac Impedance spectra of two half-charged lithium-ion cells and their resultant symmetric cells measured immediately after charging: (a) spectra of source cells (diamond marker (◇): $OCV = 3.457$ V; square marker (□): $OCV = 3.473$ V); (b) spectrum of symmetric cathode cell ($OCV = 4$ mV); (c) spectrum of symmetric anode cell ($OCV = 22$ mV); and (d) summation spectra of the source cells (◇) and symmetric cells (□). Frequencies are indicated for the solid markers.

formation of surface layers on carbon anodes has been studied quite extensively [13,14] with structural analysis techniques. The reduction of electrolyte salt and organic solvent may lead to the precipitation of some insoluble lithium salts, e.g. LiF, $ROCO_2Li$ or $Li_2CO_3$, on the lithiated carbon surface. Some of these reactions consume the electrolyte $LiPF_6$, and hence, $R_s$ should also increase with the time. As the thickness of the surface layer increases, the associated capacitance, $C_f$, is expected to decrease, exactly as observed in this experiment (Fig. 11b). However, the value of $R_sC_s$ is not constant, but rather decreases with time. This implies that the surface layers is not uniform either in composition (e.g. the outer surface layers have lower dielectric constants) or in structure (e.g. outer layers are porous). The charge-transfer resistance, $R_{ct}$, increases in general with storage time, but decreases a little from day 2 to 4. The explanation for this $R_{ct}$ change will be discussed in the following section.

The impedance spectra of the symmetric cathode cell (Fig. 9) cannot be modeled well with the circuit in Fig. 10a, since they clearly consist of more than two semicircles. Therefore, a third $RQ$ pair is introduced to account for the

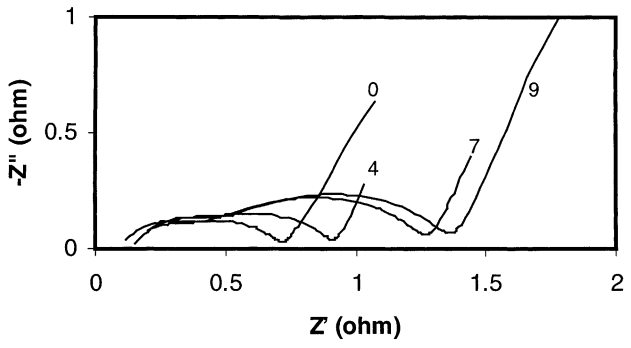


Fig. 8. An ac impedance spectra of the symmetric anode cell (Fig. 7c) as a function of storage time.

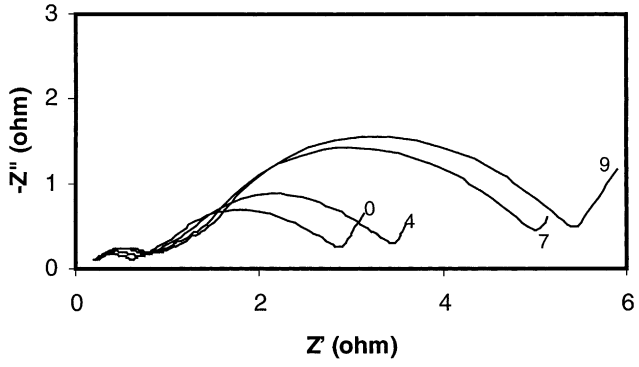


Fig. 9. An ac impedance spectra of the symmetric cathode cell (Fig. 7b) as a function of storage time.

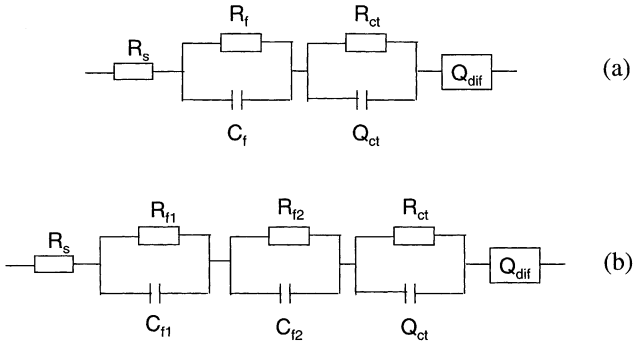


Fig. 10. Equivalent circuits for (a) the symmetric anode cell and (b) the symmetric cathode cell.

possibility that two different surface layers may co-exist. This equivalent circuit can model the cathode spectra with good accuracy. The data-fitting results are shown in Fig. 12. It can be seen that the electrolyte solution resistance, $R_s$, hardly changes or even slightly decreases during storage, a pattern which differs from that the symmetric anode cell, in which $R_s$ increases with storage time. In addition, the surface layer resistances, $R_{f1}$ and $R_{f2}$, are substantially larger than $R_s$, while $R_f$ and $R_s$ are very close in the anode cell. These differences suggest that the surface layers on the $Li_{1-x}Ni_{0.8}Co_{0.2}O_2$ cathode are very likely different in nature from the surface layers on the lithiated carbon anode. There is a possibility that the transition metal ions $Co^{2+}$ and $Ni^{2+}$ are dissolved in the electrolyte solution from $Li_{1-x}Ni_{0.8}Co_{0.2}O_2$ via disproportionation under the presence of HF, similar to the case of $Li_{1-x}Mn_2O_4$ [15]. The $Co^{2+}$ and $Ni^{2+}$ may react with $F^-$ to form $CoF_2$ and $NiF_2$ precipitates on the cathode

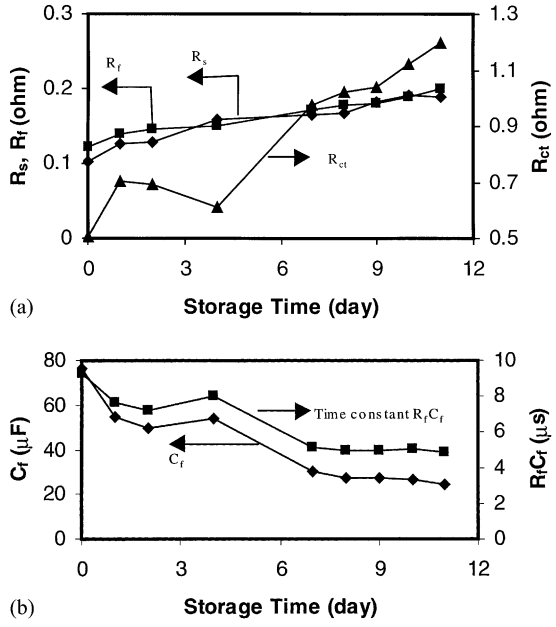


Fig. 11. Fitting results for the symmetric anode cell as a function of storage time: (a) resistance parameters and (b) surface-layer capacitance.

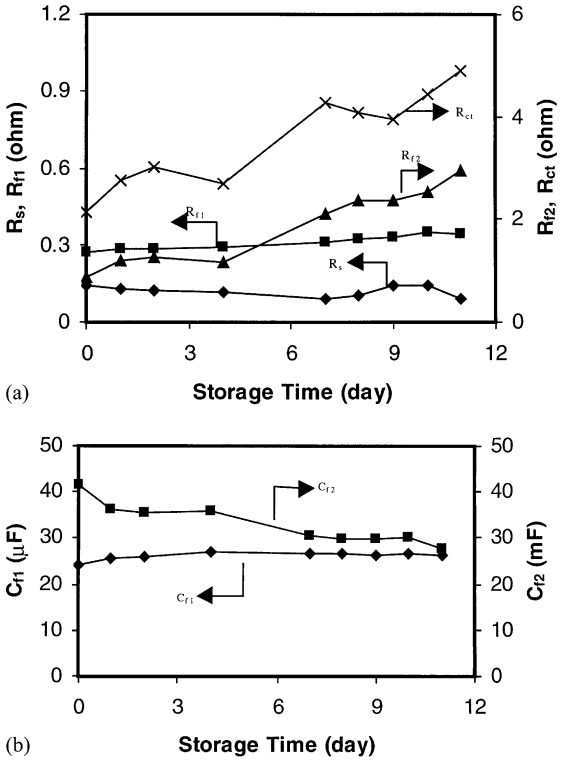


Fig. 12. Fitting results for the symmetric cathode cell as a function of storage time: (a) resistance parameters and (b) capacitance parameters.

surface. Another possibility is the oxidation of the organic solvent (EC or DEC) by the strongly oxidizing $Ni^{4+}$ and $Co^{4+}$ to form amorphous polymer layers on the surface [16]. Neither mechanism decreases the $LiPF_6$ concentration in the electrolyte, and hence, neither should affect $R_s$.

Fig. 12a also shows that resistance of the first surface layer, $R_{f1}$, remains almost unchanged during storage and is significantly smaller than that of the second surface layer, $R_{f2}$, which increases with time. Consistent with the change in resistance, $C_{f1}$ is almost unchanged during storage, while $C_{f2}$ decreases with time. This means that only the second surface layer becomes thicker after the symmetric cell is assembled. Since $C_{f2}$ is surprisingly large (on the order of 10 mF), while $R_{f2}$ is sizable (about 2 Ω), the second surface layer must be very thin but extremely insulating to lithium-ion conduction. An organic polymer layer may meet these two conditions. As for the first surface layer, it might be composed of lithium salt because $R_{f1}$ is small (about 0.15 Ω) and $C_{f1}$ is on the order of 10 μF. The charge-transfer resistance, $R_{ct}$, increases during storage, which is similar to the case of the symmetric anode cell. $R_{ct}Q_{ct}$ is obviously the source of the large semicircle at medium to low frequencies in the spectra.

### 3.3. Charge-transfer process

As shown in Figs. 11a and 12a, the charge-transfer process plays an important role in the lithium-ion transport in a lithium-ion cell. Levi et al. proposed that the charge-

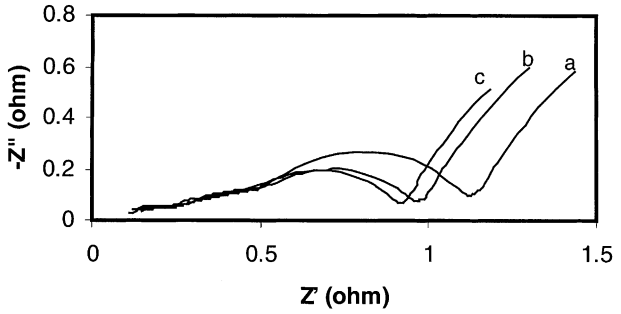


Fig. 13. An ac impedance spectra of three fully charged lithium-ion cells using different solvents in the electrolyte solutions: (a) EC:DEC; (b) 2EC:DEC:2DMC; (c) EC:4EMC. The electrode area was 20.3 $cm^2$.

transfer process on the cathode side takes place at the interface between the surface layer and the cathode particles [10]. This means that, once the surface layer is formed, the charge-transfer resistance, $R_{ct}$, should not change with the growth of the surface layer as long as the composition in the vicinity of the interface does not change. However, the proceeding data analysis indicates that $R_{ct}$ increases with time in the beginning period of storage, although this change will stop after about 3 weeks (Fig. 1). Moreover, it can also be inferred from Levi's model that the charge-transfer capacitance should be independent of the type of electrolyte solution if a surface layer of the same composition covers the active electrode particles. This inference is inconsistent with our experimental results for cells using three different electrolyte solutions, as shown in Fig. 13.

Fig. 14 shows the impedance spectra of two source cells using different electrolytes and their corresponding symmetric cells. Since the source cells have been stored for 17 days, surface layers presumably cover all of the electrodes. According to the analysis given in the preceding sections, the charge-transfer resistances on the cathode side are about 4 Ω for the cell using EC:DEC solvent and 2 Ω for the cell using 2EC:DEC:2DMC solvent (Fig. 14a). If the charge-transfer does not involve the electrolyte solution, the charge-transfer resistance of the symmetric cathode cell made from these two source cells would be about 6 Ω. However, it was measured to be about 4 Ω, which is about twice the cathode charge-transfer resistance (2 Ω) for a cell using the same solvent 2EC:DEC:2DMC. Therefore, the electrolyte solution is certainly involved in the charge-transfer process. One possible mechanism could be that the surface layers on the cathode are not completely electronically insulating, i.e. they may be mixed conductors of lithium-ion and electron. Because these layers are so thin, they allow lithium ions and electrons to move through rather fast even though the ionic and electronic conductivity might be very small. In this situation, the charge-transfer process takes place at the interface between the surface layers and the electrolyte solution. Therefore, physical properties such as the wetability of the solvent and the lithium-ion concentration of the electrolyte may affect the charge-transfer resistance.

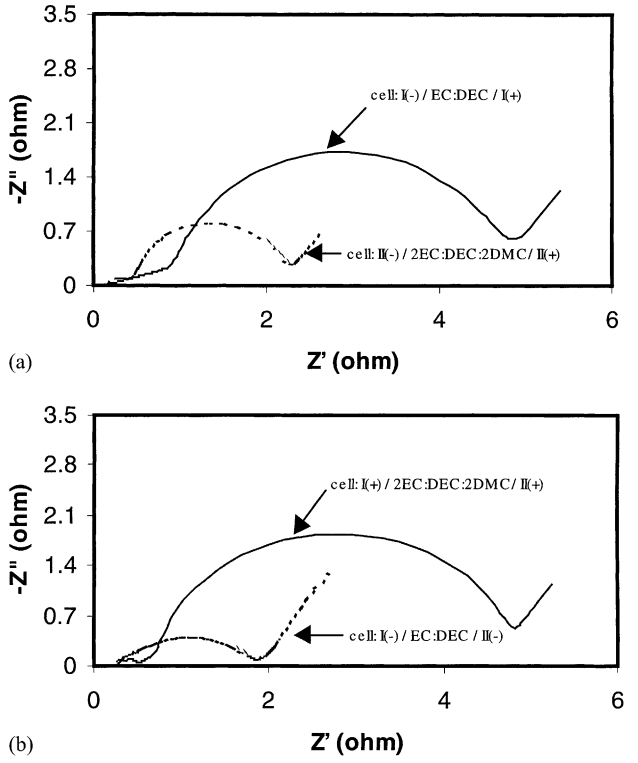


Fig. 14. An ac impedance spectra of (a) two fully charged cells using different solvents and (b) their resultant symmetric cells. The structures of the cells are given in the plots.

## 4. Conclusions

The impedance of Argonne high-power lithium-ion cells has been found to increase in the beginning period of storage, but stabilize in about 3 weeks. A new approach based on the use of symmetric cells was developed to permit the electrochemical processes on the anode side and the cathode side to be studied separately. The cathode-side impedance, especially the charge-transfer resistance, is the main contributor to the cell impedance and to its rise during storage. It is proposed that this charge-transfer process takes place at the interface between the electrolyte solution and the surface of the surface layers, which are thought to be electron-lithium-ion mixed conductors. Charge-transfer resistance is also the main component of anode-side impedance. The nature of the surface layers on the anode is likely different from that of the surface layers on the cathode. Future research should focus on the cathode side to minimize the cell impedance and improve its stability.

## Acknowledgements

This study was financially supported by US Department of Energy, Office of Advanced Transportation Technology, under Contract W-31-109-Eng-38. We would like to thank

Dr. D.W. Dees for helpful discussion and his assistance with impedance measurement.

## References

[1] J.N. Reimers, J.R. Dahn, J. Electrochem. Soc. 139 (1992) 2091.
[2] K. Sawai, T. Ohzuku, T. Hirai, Chem. Express 5 (1990) 837.
[3] T. Ohzuku, A. Ueda, M. Nagayama, Y. Iwakoshi, H. Komori, Eletrochim. Acta 38 (1993) 1159.
[4] G. Pistoia, A. Antonini, R. Rosati, D. Zane, Electrochim. Acta 41 (1996) 2683.
[5] A.G. Ritchie, C.O. Giwa, J.C. Lee, P. Bowles, A. Gilmour, J. Allan, J. Power Sources 80 (1999) 128.
[6] M. Saft, G. Chagnon, T. Faugeras, G. Sarre, P. Morhet, J. Power Sources 80 (1999) 180.
[7] K. Amine, Report to US Department of Energy, 1998, unpublished.
[8] C.H. Chen, J. Liu, K. Amine, Electrochem. Solid-State Lett., in press.
[9] D. Aurbach, A. Zaban, J. Electrochem. Soc. 141 (1994) 118.
[10] M.D. Levi, G. Salitra, B. Markovsky, H. Teller, D. Aurbach, U. Heider, L. Heider, J. Electrochem. Soc. 146 (1999) 1279.
[11] D. Aurbach, M.D. Levi, E. Levi, H. Teller, B. Markovsky, G. Salitra, U. Heider, L. Heider, J. Electrochem. Soc. 145 (1998) 3024.
[12] J.R. Macdonald, Impedance Spectroscopy, Wiley/Interscience, New York, 1987.
[13] D. Aurbach, A. Zaban, Y. Ein-Eli, I. Weissman, O. Chusid, B. Markovsky, M. Levi, E. Leci, A. Schechter, E. Granot, J. Power Sources 68 (1997) 91.
[14] O. Chusid, Y. Ein-Eli, D. Aurbach, M. Babai, Y. Carmeli, J. Power Sources 43-44 (1993) 47.
[15] A. Blyr, C. Sigala, G. Amatucci, D. Guyomard, Y. Chabre, J.M. Tarascon, J. Electrochem. Soc. 145 (1998) 194.
[16] M.G.S.R. Thomas, P.G. Bruce, J.B. Goodenough, J. Electrochem. Soc. 132 (1985) 1521.